The NLRP3 Inflammasome Has a Critical Role in Peritoneal Dialysis-Related Peritonitis

Nicolas Hautem, Johann Morelle, Amadou Sow, Cyril Corbet, Olivier Feron, Eric Goffin, François Huaux and Olivier Devuyst

Supplementary Material

DETAILED MATERIAL AND METHODS

Human peritonitis and samples collection. Peritoneal effluent was collected (first cloudy bag) in PD patients with peritonitis (defined as cloudy dialysate containing >100 WBC/mm³ and/or at least 50% of PMN) and PD controls.[1] The purification of leukocytes from the peritoneal effluent was achieved through centrifugation (1000 rpm at 4°C for 10min) followed by fluorescence-associated cell sorting (FACS) (BD FACS Aria III Cell Sorter, BD, San Jose, CA) using a rat anti-human CD45 antibody (BD Biosciences, Erembodegem, Belgium), as previously reported.[2] The technique yields a high quality purification of cells present in the peritoneal effluent, with 99.9% of remaining cells after purification being leukocytes. The leukocyte pellet was finally collected in RNA lysis buffer (Applied Biosystems, Thermo Fischer Scientific, Waltham, MA). The CRP levels were measured in the serum by immunonephelometry using a BN II analyzer (Dade Behring, Deerfield, USA). A peritoneal biopsy was obtained at the time of catheter withdrawal in a patient with refractory peritonitis, and in PD controls at the time of transplantation or transfer to hemodialysis, in agreement with ethical committee. The use of human biopsy samples and dialysate was approved by the Ethical Review Board of Saint-Luc Academic Hospital (Brussels, Belgium).

Experimental animals and mouse models of peritonitis. The experiments were conducted using gender-matched C57BL/6J wild-type and *Nalp3* mice, aged 11-16 weeks. The wild-type mice were obtained from Charles Rivers (Brussels, Belgium). *Nalp3* mice were generated as described previously,[3] and obtained from B. Ryffel (Université d'Orleans, Orleans, France). Animals were housed in an air-conditioned room with a 12/12-h dark-light cycle and acclimated for 1 week before the experiment. Mice were allowed free access to standard laboratory diet (Scientific animal food & engineering, Augy, France) and tap water.
Acute peritonitis was induced by either a single i.p. injection of lipopolysaccharide (LPS, 10 mg/kg, *E. coli* serotype O111: B4; Sigma-Aldrich, Buchs, Switzerland), or repeated i.p. injections (on days 1 and 5) of 10^9/ml *E. Coli* (ATCC-25992) diluted in 2ml of 3.86% glucose-based dialysis solution (Dianeal, Baxter, Nivelles, Belgium). In experiments using anakinra (Kineret®, Sobi, Brussels, Belgium), the drug was injected i.p. at the dose of 50 mg/kg/day,[4] starting from day 1 or day 2 (delayed anakinra protocol). Ceftazidime was started 24h after the bacterial injection at a daily i.p. dose of 40 mg/kg, from day 2 to day 5.
The rationale for showing infiltration of neutrophils and WBC in models of LPS- and *E. coli*-induced peritonitis respectively is based on previous studies demonstrating that a persistent

(>48h) inflammatory stress leads to a switch in white blood cells populations infiltrating the injured peritoneal tissue, with an early (within 6 h) infiltration by polymorphonuclear neutrophils being progressively replaced by macrophages and lymphocytes after 48-72h.[5] As a result, a unique LPS injection is followed by an isolated rise in neutrophils in the peritoneal effluent, while the resolution of the inflammatory stress prevents the switch in peritoneal infiltrate.[6] On the contrary, a 6-day exposure of the membrane to *E. coli* (repeated injections) leads to an initial recruitment of neutrophils and their progressive replacement by mononuclear cells after 48-72 h.[7]
The experiments were conducted in accordance with the National Research Council Guide for the Care and Use of Laboratory Animals and approved by the ethics committee of the Université catholique de Louvain Medical School (Brussels).

Uremic mouse models. Tubulointerstitial nephropathy was induced by dietary adenine in C57BL6 mice, as previously reported.[8] Briefly, mice in the adenine group received standard laboratory diet (Scientific animal food & engineering) to which 0.25% adenine and 20% casein were added. Sham animals received the same diet without adenine. The addition of adenine to the diet of mice during 3 weeks led to the development of intra-tubular casts, tubulointerstitial damage, and severe uremia as reported previously.[9]
Knock-in mice harbouring a missense human mutation of *UMOD* ($Umod^{mut/mut}$) and control littermates ($Umod^{wt/wt}$) were obtained from the University of Zurich, Zurich, Switzerland. The $Umod^{mut/mut}$ mice recapitulate the features of uromodulin-associated kidney disease, with progressive inflammatory cell infiltration, tubule dilation, tubulointerstitial fibrosis and mild renal failure, as previously reported.[10,11]

Bactericidal clearance. The bactericidal clearance was evaluated by counting the number of colony forming units (CFU) of *E. coli* in the peritoneal effluent. Repeated serial dilutions were made and 10 µl of each bacterial concentration were added on a non-selective agar medium. After overnight incubation at 37°C, the counting of CFU allowed to determine the number of *E. coli* in the peritoneal effluent.[12]

Peritoneal transport studies, tissue sampling. A peritoneal equilibration test was used to investigate peritoneal transport parameters in mice as previously described.[13] Blood samples were collected from the inferior vena cava. Plasma was stored at -20°C until analysis. Urea, glucose and sodium were assayed using Kodak Ektachem DT60 II and DTE II analysers

(Eastman Kodak Company, Rochester, NY). Proteins concentration was assayed using Pierce BCA protein assay kit (Thermo scientific, Rockford, IL). Visceral peritoneum carefully dissected from the mesentery was snap-frozen in liquid nitrogen and stored at -80°C, or routinely fixed in 4% paraformaldehyde in 0.1 M phosphate buffer (VWR, Brussels, Belgium). The differential cells count in the dialysate was performed by using the differential cell counter MS9-3v (Melet Schloesing laboratoires, Osny, France).

Fluorescence-activated cell sorting. Fluorescent surface labelling of cells from dialysate were performed using antibodies rat anti-mouse CD45, CD11b and GR1 (BD Biosciences). Cells fixed in 1.25% paraformaldehyde were analyzed in a FACSCanto II (Becton Dickinson) by using FlowJo software (Ashland, OR).

RT-PCR and semiquantitative real-time RT-PCR. Total RNA from mouse visceral peritoneum was extracted with Trizol (Invitrogen, Merelbeke, Belgium) and using AurumTM Total RNA fatty and fibrous tissue kit (Bio-Rad, Hercules, CA) according to the manufacturer's protocol. DNase I treatment was performed to eliminate genomic DNA contamination. Total RNA was extracted from total leukocytes with RNAqueousR kit (Applied Biosystems), following the manufacturer's protocol. One microgram of RNA was used to perform the reverse transcriptase reaction with iScriptTM cDNA Synthesis Kit (Bio-Rad). Changes in target genes mRNA levels were determined by semiquantitative reverse-transcriptase-polymerase chain reaction with an iCycler IQ system (Bio-Rad) using SYBR Green I detection as described previously.[13] The PCR conditions were 95°C for 3min followed by 40 cycles of 30s at 95°C, 15s at 60°C and 1 min at 72°C. The relative changes in Target mRNA /GAPDH mRNA ratios between vehicle and treated groups were determined by using the relation $2^{-\Delta\Delta Ct}$.

Antibodies. The following antibodies were used in this study: rabbit anti-human CD11b (Abcam, Cambridge, UK); rat anti-human NALP3 (R&D Systems, Wiesbaden-Nordenstadt, Germany); rat anti-mouse CD31 (Santa Cruz Biotechnology, Santa Cruz, CA); rabbit anti-mouse α-SMA (Abcam); rabbit anti-mouse NALP3 (Abcam); mouse anti- iNOS (BD transduction laboratories, Lexington, KI); mouse anti-eNOS (BD transduction laboratories); goat anti-mouse IL-1R1 (R&D Systems); rat IgG2A and goat IgG isotype controls (R&D Systems); and mouse anti- β-actin (Sigma, St Louis, MO, USA).

Western blotting. Immunoblotting were performed as described.[14] Proteins were extracted from visceral peritoneum, lysed in buffer containing protease inhibitors (Complete Mini, Roche Diagnostics, Belgium), followed by sonication and centrifugation at 10,000 rpm for 10 min at 4°C. Proteins were diluted in Laemmli buffer and separated by SDS-PAGE. After blotting on nitrocellulose membrane and blocking for 30min, membrane was incubated overnight at 4°C with primary antibody, washed, incubated with peroxidase-labeled secondary antibody for 1 hour, and visualized with enhanced chemiluminescence (ECL Pierce). Densitometry analysis was performed by scanning the blots and measuring the relative density of each band normalized to β-actin using the ImageJ software.

Enzyme-linked immunosorbent assays. ELISA kits were used to measure IL-1β, IL-6 and TNF α (R&D Systems, Wiesbaden-Nordenstadt, Germany). Assays were run according to the manufacturer's protocols.

Determination of Nitrite/Nitrate (NOx). The production of nitrite and nitrate in the dialysate was measured using a colorimetric assay (Cayman Chemical, Ann Arbor, Michigan, USA). After 3h incubation with nitrate reductase and NADPH at room temperature, total nitrite concentration in the samples was measured by the Griess reaction at 540 nm.

Tissue staining and immunohistochemistry. Samples from the visceral and parietal peritoneum were fixed in 4% paraformaldehyde and embedded in paraffin. The embedded tissue was sectioned at 6μm. Masson's trichrome staining and immunostaining were performed as previously described.[13-15] Sections were scanned by SCN4000 scanner (Leica, Heerbrugg, Switzerland) and visualized by digital image hub (Leica) viewed under a Leica DMR coupled to a Leica DC 300 camera.

Immunofluorescence. Samples from the visceral peritoneum were treated as described above.[15,16] The sections were dewaxed, and rehydrated in ethanols and blocked with blocking serum. The tissue were incubated for 2h with primary antibody, washed three times in PBS, incubated for 1h with the secondary (Alexa labelled) antibody, Sections were subsequently mounted in Prolong Gold anti-fade reagent (Invitrogen) and analyzed under a Zeiss LSM 510 Meta Confocal microscope (Carl Zeiss, Jena, Germany). The specificity of the immunostaining for CD31 and IL-1R1 was confirmed by negative controls including the use

of isotype controls (used at same concentration than original antibodies) and of antibodies against the α-smooth muscle actin as an unrelated marker (see Suppl. Fig. 1).

Cell culture. Human umbilical vein endothelial cells (HUVEC) were used within 6 months of purchase from Sigma, acting as a distributor for ECACC (European Collection for Cell Culture). HUVECs were routinely cultured in endothelial cell growth medium (Cell Applications) and used between passages 2 and 5. Proliferation assays was performed using PrestoBlue® Cell Viability Reagent (ThermoFisher scientific, Rockford, IL) according to the manufacturer's protocol.

Vascular permeability and tube formation assays. Vascular permeability was assessed on HUVEC monolayers treated for 19h with 100 ng/ml IL-1β in absence or presence of 1 mg/ml anakinra by using the Fluorescein isothiocyanate (FITC)-dextran leakage vascular permeability assay (Merck Millipore, Darmstadt, Germany) according to the manufacturer's instructions. The formation of capillary-like endothelial tubes was determined using an in vitro assay by plating HUVECs on growth factor-reduced Matrigel (BD Biosciences). Cells were treated for 6h with 10ng/ml IL-1 β in absence or presence of 1mg/ml anakinra. Cumulative tube length and number of junctions were determined by using the angiogenesis analyzer for ImageJ software (https://imagej.nih.gov/ij/).

Data analysis. Results were expressed as mean ± SEM. Differences between groups were assessed by unpaired Student's t-test or one-way ANOVA followed by Bonferroni's multiple comparisons test (GraphPad Software, San Diego, California, USA), as appropriate. $P< 0.05$ was considered statistically significant.

SUPPLEMENTARY FIGURES

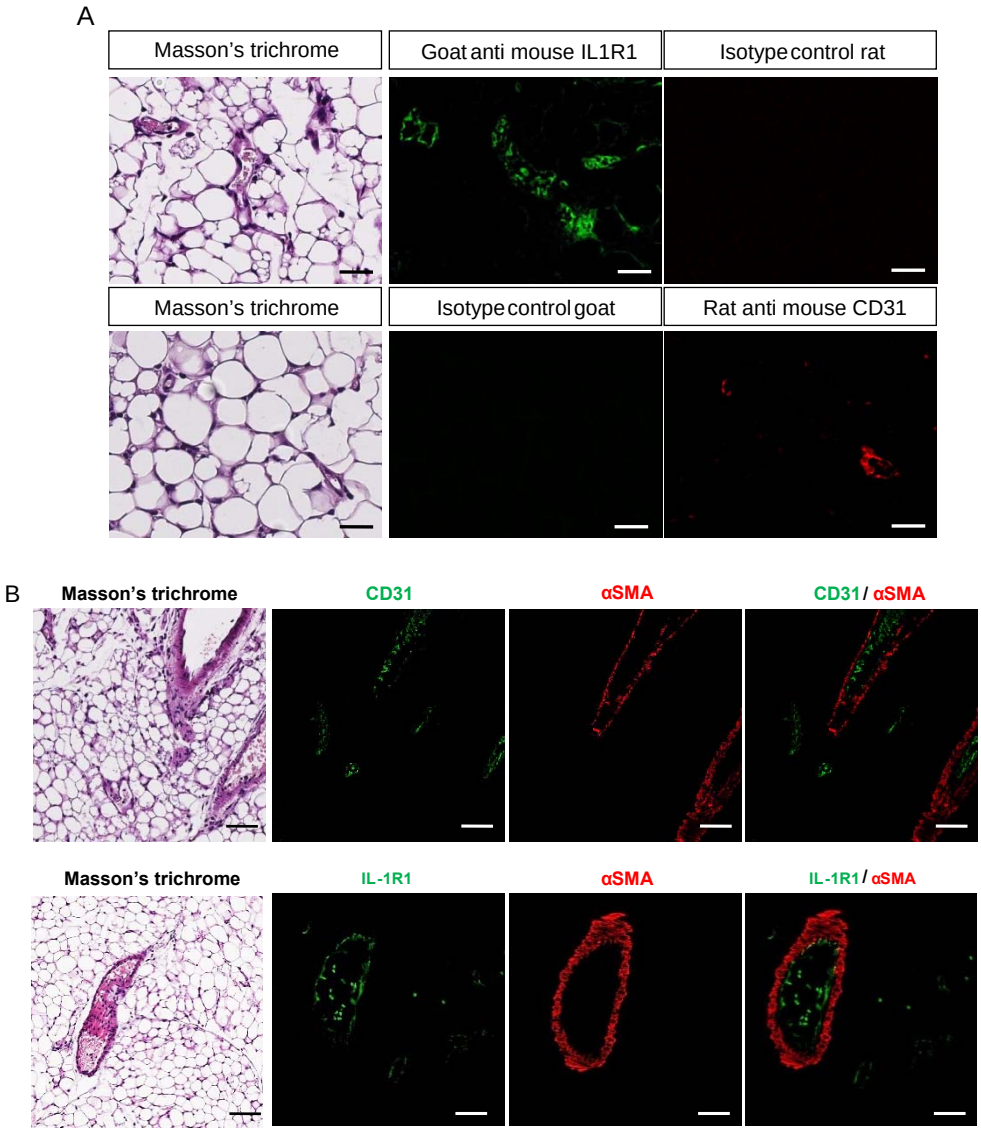

Suppl. Fig 1. Specificity of the CD31 and IL-1R1 immunostaining.
(**A**) Representative sections of control mouse visceral peritoneum stained with Masson's trichrome and immunofluorescence using anti- IL-1R1 and anti-CD31 antibodies or specific isotype controls. IL-1R1 antibody (green channel) shows a specific staining expressed on endothelial cells and mononuclear cells in the lumen of vessels. CD31 antibody (red channel) shows a specific staining limited to endothelium. Respective isotype controls for each antibody are negative. Scale bars: 50 µm. Magnification, 40x.
(**B**) Representative sections of visceral peritoneum from LPS-treated mice stained with Masson's trichrome and anti- CD31 or anti-IL-1R1 (green channel) and anti-α-smooth muscle actin (αSMA) (red channel) as unrelated marker. The merge images show that αSMA is localized in smooth muscle cells of vessels wall and not expressed in $CD31^{+}$ endothelium. Note that IL-1R1 is expressed on both inflammatory and endothelial cells. Scale bars, 50µm. Magnification, 20x.

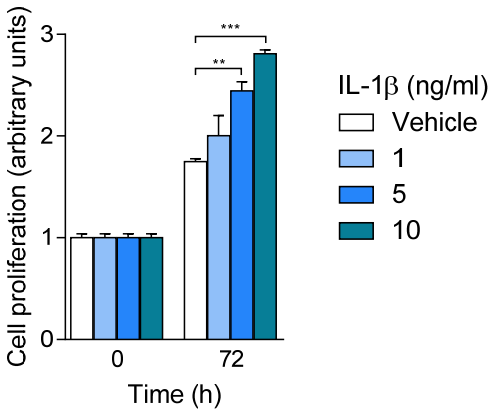

Suppl. Fig 2. Effect on IL-1β on endothelial cell proliferation.
IL-1β induces a dose- and time-dependent increase of the proliferation of human umbilical vein endothelial cells (PrestoBlue® Cell Viability Reagent). The increase is statistically significant for IL-1β concentrations ≥5 ng/ml after 72h (n=6 for each concentration).
** $p<0.01$; *** $p<0.001$.

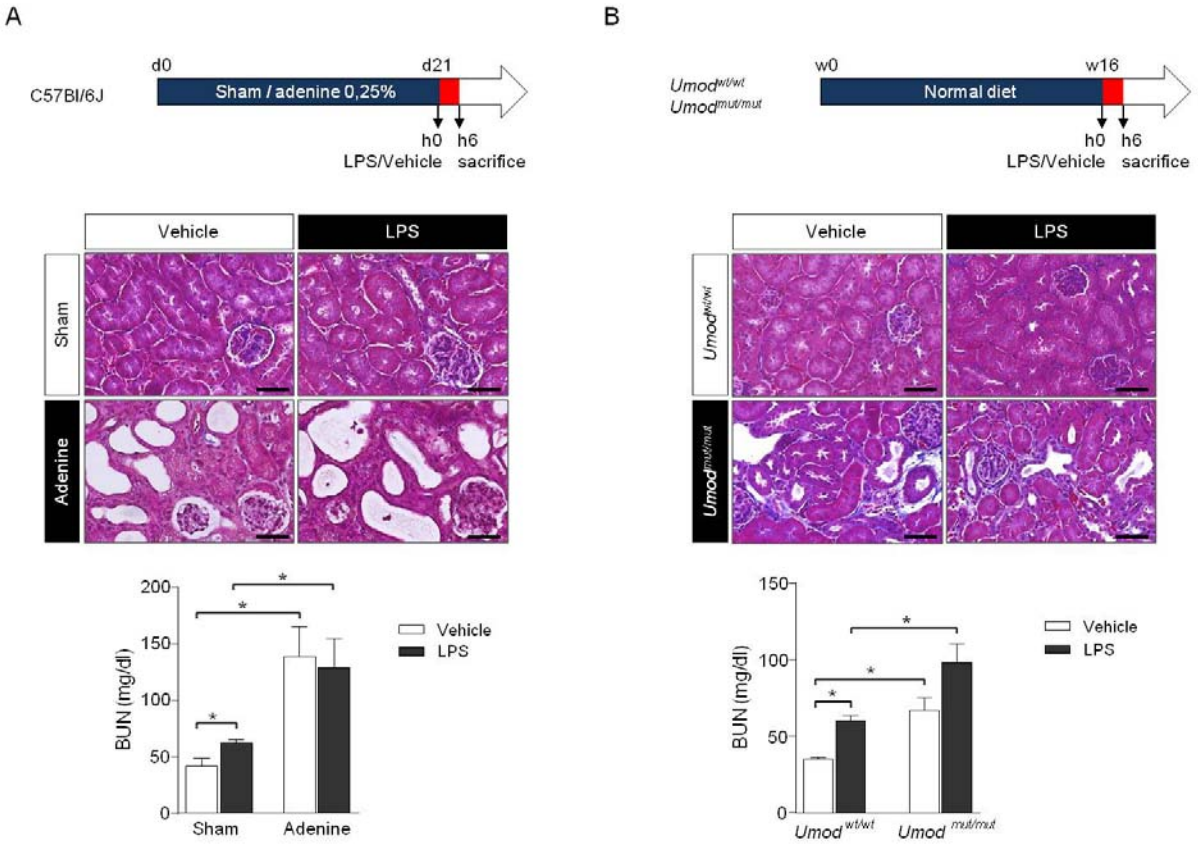

Suppl. Fig 3. Mouse models of chronic kidney disease with LPS-induced peritonitis.
(**A**) Control mice or mice with tubulointerstitial nephropathy induced by dietary adenine were i.p. injected with LPS or vehicle on day 21. Adenine diet induced tubule dilation, tubular casts, enlargement of Bowman's space, and increased the level of blood urea nitrogen (BUN), as compared with sham animals. LPS did not further affect kidney structure or function (n=4 mice per group). * $p<0.05$. (**B**) Mice harbouring a homozygous missense mutation of *Umod* (*Umod*$^{mut/mut}$) and control littermates (*Umod*$^{wt/wt}$) were i.p. injected with LPS or vehicle to induce peritonitis. The *Umod*$^{mut/mut}$ mice show typical features of uromodulin-associated kidney disease including tubulointerstitial lesions (casts, dilatations) and increased levels of BUN at week 16 of age. The injection of LPS did not change the structure of kidneys but significantly increased the BUN levels in both groups (n=3 mice per group).
* $p<0.05$. Scale bars, 50 µm.

Suppl. Table 1. Effect of delayed anakinra on peritoneal transport during *E. coli*-induced peritonitis.

Groups	n	MTAC urea (µl/min)	Dialysate albumin (mg/ml)	Net UF/BW (µl/g)
Vehicle	5	16.5 ± 0.8	2.3 ± 0.0	53.0 ± 3.4
E. coli + vehicle	5	42.6 ± 2.1 [a]	3.6 ± 0.1 [a]	11.3 ± 4.2 [a]
E. coli + anakinra	5	30.6 ± 1.3 [a,b]	3.1 ± 0.0 [a,b]	31.0 ± 2.4 [a, b]

Anakinra was started 24h after i.p. injection of *E. coli* (i.e. on day 2) and pursued until day 5.

Abbreviations: MTAC, mass transfer area coefficient; UF, ultrafiltration; BW, body weight

[a] $p<0.05$ *vs* vehicle; [b] $p<0.05$ *vs E. coli* + vehicle

Suppl. Table 2: Primers used for quantitative RT-PCR analyses.

Gene products	Forward primers (5'-3')	Reverse primers (5'-3')	PCR products (bps)	Efficiency
ASC	TGGATGCTCTGTACGGGAAG	CCAGGCTGGTGTGAAACTGAA	110	1.01 ± 0.02
NALP3	CGTGAGTCCCATTAAGATGGAGT	CCCGACAGTGGATATAGAACAGA	191	0.99 ± 0.01
CASPASE-1	CGCAGATGCCCACCACT	TGCCCACAGACATTCATACAG	96	0.97 ± 0.03
PYRIN	TAAGACCCCTAGTGACCATCTG	TTCCCCATAGTAGGTGACCAG	184	1.03 ± 0.01
GAPDH	ACAACTTTGGTATCGTGGAAGG	GCCATCACGCCACAGTTTC	101	1.04 ± 0.02
IL-1β	ATGATGGCTTATTACAGTGGCAA	GTCGGAGATTCGTAGCTGGA	132	0.98 ± 0.04
Nalp3	ATCAACAGGCGAGACCTCTG	GTCCTCCTGGCATACCATAGA	96	1.02 ± 0.02
Il-1β	GAAATGCCACCTTTTGACAGTG	TGGATGCTCTCATCAGGACAG	116	0.99 ± 0.03
Inos	GTTCTCAGCCCAACAATACAAGA	GTGGACGGGTCGATGTCAC	127	1.00 ± 0.04
Enos	TCAGCCATCACAGTGTTCCC	ATAGCCCGCATAGCGTATCAG	87	1.01 ± 0.02
Gapdh	TGCACCACCAACTGCTTAGC	GGATGCAGGGATGATGTTCT	176	1.04 ± 0.03

REFERENCES

1. Warady BA, Schaefer F, Holloway M, et al: Consensus guidelines for the treatment of peritonitis in pediatric patients receiving peritoneal dialysis. *Perit Dial Int* 20: 610-24, 2000
2. Beliakova-Bethell N, Massanella M, White C, et al: The effect of cell subset isolation method on gene expression in leukocytes. *Cytometry* 85: 94-104, 2014
3. Martinon F, Pétrilli V, Mayor A, Tardivel A, Tschopp J: Gout-associated uric acid crystals activate the NALP3 inflammasome. *Nature* 440: 237-241, 2006
4. Sgroi A, Gonelle-Gispert C, Morel P, et al: Interleukin-1 receptor antagonist modulates the early phase of liver regeneration after partial hepatectomy in mice. *PLoS One* 6: e25442, 2011
5. Jones SA: Directing transition from innate to acquired immunity: defining a role for IL-6. *J Immunol* 175: 3463-8, 2005
6. Ni J, McLoughlin RM, Brodovitch A, et al: Nitric oxide synthase isoforms play distinct roles during acute peritonitis. *Nephrol Dial Transplant* 25: 86-96, 2010
7. Yung S, Chan TM: Pathophysiological changes to the peritoneal membrane during PD-related peritonitis: the role of mesothelial cells. *Mediators Inflamm* 2012:484167, 2012
8. Santana AC, Degaspari S, Catanozi S, et al: Thalidomide suppresses inflammation in adenine-induced CKD with uraemia in mice. *Nephrol Dial Transplant* 28: 1140-9, 2013
9. Jia T, Olauson H, Lindberg K, et al: A novel model of adenine-induced tubulointerstitial nephropathy in mice. *BMC Nephrol* 14: 116, 2013
10. Bernascone I, Janas S, Ikehata M, et al: A transgenic mouse model for uromodulin-associated kidney diseases shows specific tubulo-interstitial damage, urinary concentrating defect and renal failure. *Hum Mol Genet* 19: 2998-3010, 2010
11. Eckardt KU, Alper SL, Antignac C, et al: Autosomal dominant tubulointerstitial kidney disease: diagnosis, classification, and management-A KDIGO consensus report. *Kidney Int* 88: 676-83, 2015
12. Buijs J, Dofferhoff AS, Mouton JW, Wagenvoort JH, van der Meer JW: Concentration-dependency of beta-lactam-induced filament formation in Gram-negative bacteria. *Clin Microbiol Infect* 14:344-9, 2008
13. Ni J, Cnops Y, McLoughlin RM, Topley N, Devuyst O: Inhibition of nitric oxide synthase reverses permeability changes in a mouse model of acute peritonitis. *Perit Dial Int* 3: 11-14, 2005
14. Ni J, Moulin P, Gianello P, Feron O, Balligand JL, Devuyst O: Mice that lack endothelial nitric oxide synthase are protected against functional and structural modifications induced by acute peritonitis. *J Am Soc Nephrol* 14: 3205-3216, 2003
15. Combet S, Van Landschoot M, Moulin P, et al: Regulation of aquaporin-1 and nitric oxide synthase isoforms in a rat model of acute peritonitis. *J Am Soc Nephrol* 10: 2185-2196, 1999
16. Morelle J, Sow A, Hautem N, et al: Interstitial Fibrosis Restricts Osmotic Water Transport in Encapsulating Peritoneal Sclerosis. *J Am Soc Nephrol* 26: 2521-33, 2015